*Biology of Reproduction,* 2021, 105(4), 1043–1055
https://doi.org/10.1093/biolre/ioab082
Research Article
Advance Access Publication Date: 18 May 2021



Research Article

# Evolutionary, proteomic, and experimental investigations suggest the extracellular matrix of cumulus cells mediates fertilization outcomes†

**Sara Keeble[1], Renée C. Firman[2], Brice A. J. Sarver[3], Nathan L. Clark[4], Leigh W. Simmons[2] and Matthew D. Dean[1,*]**

[1]Molecular and Computational Biology, Department of Biological Sciences, University of Southern California, Los Angeles, California, USA, [2]Centre for Evolutionary Biology, School of Biological Sciences (M092), University of Western Australia, Australia, [3]Division of Biological Sciences, University of Montana, Missoula, Montana, USA and [4]Department of Human Genetics, University of Utah, Salt Lake City, Utah, USA

*__Correspondence:__ Molecular and Computational Biology, University of Southern California, 1050 Childs Way, Los Angeles, CA 90089, USA. E-mail: matthew.dean@usc.edu

†__Grant Support:__ This project was supported by National Science Foundation CAREER award 1150259 (to M.D.D.), National Institutes of Health award 1R01GM098536 (to M.D.D.), National Science Foundation Graduate Research Fellowship (to S.K.), National Science Foundation Graduate Research Opportunities Worldwide Award (to S.K.), Society for the Study of Evolution Rosemary Grant Award (to S.K.), the Australian Research Council (to L.W.S. and R.C.F.), the University of Western Australia (to L.W.S. and S.K.), and used the UPCI Cancer Biomarkers Facility that is supported in part by award P30CA047904.

Received 27 August 2020; Revised 29 January 2021; Accepted 21 April 2021

## Abstract

Studies of fertilization biology often focus on sperm and egg interactions. However, before gametes interact, mammalian sperm must pass through the cumulus layer; in mice, this consists of several thousand cells tightly glued together with hyaluronic acid and other proteins. To better understand the role of cumulus cells and their extracellular matrix, we perform proteomic experiments on cumulus oophorus complexes (COCs) in house mice (*Mus musculus*), producing over 24,000 mass spectra to identify 711 proteins. Seven proteins known to stabilize hyaluronic acid and the extracellular matrix were especially abundant (using spectral counts as an indirect proxy for abundance). Through comparative evolutionary analyses, we show that three of these evolve rapidly, a classic signature of genes that influence fertilization rate. Some of the selected sites overlap regions of the protein known to impact function. In a follow-up experiment, we compared COCs from females raised in two different social environments. Female mice raised in the presence of multiple males produced COCs that were smaller and more resistant to dissociation by hyaluronidase compared to females raised in the presence of a single male, consistent with a previous study that demonstrated such females produced COCs that were more resistant to fertilization. Although cumulus cells are often thought of as enhancers of fertilization, our evolutionary, proteomic, and experimental investigations implicate their extracellular matrix as a potential mediator of fertilization outcomes.

## Summary sentence

Cumulus cell protein identification reveals potential roles in fertilization outcomes.

## Graphical Abstract

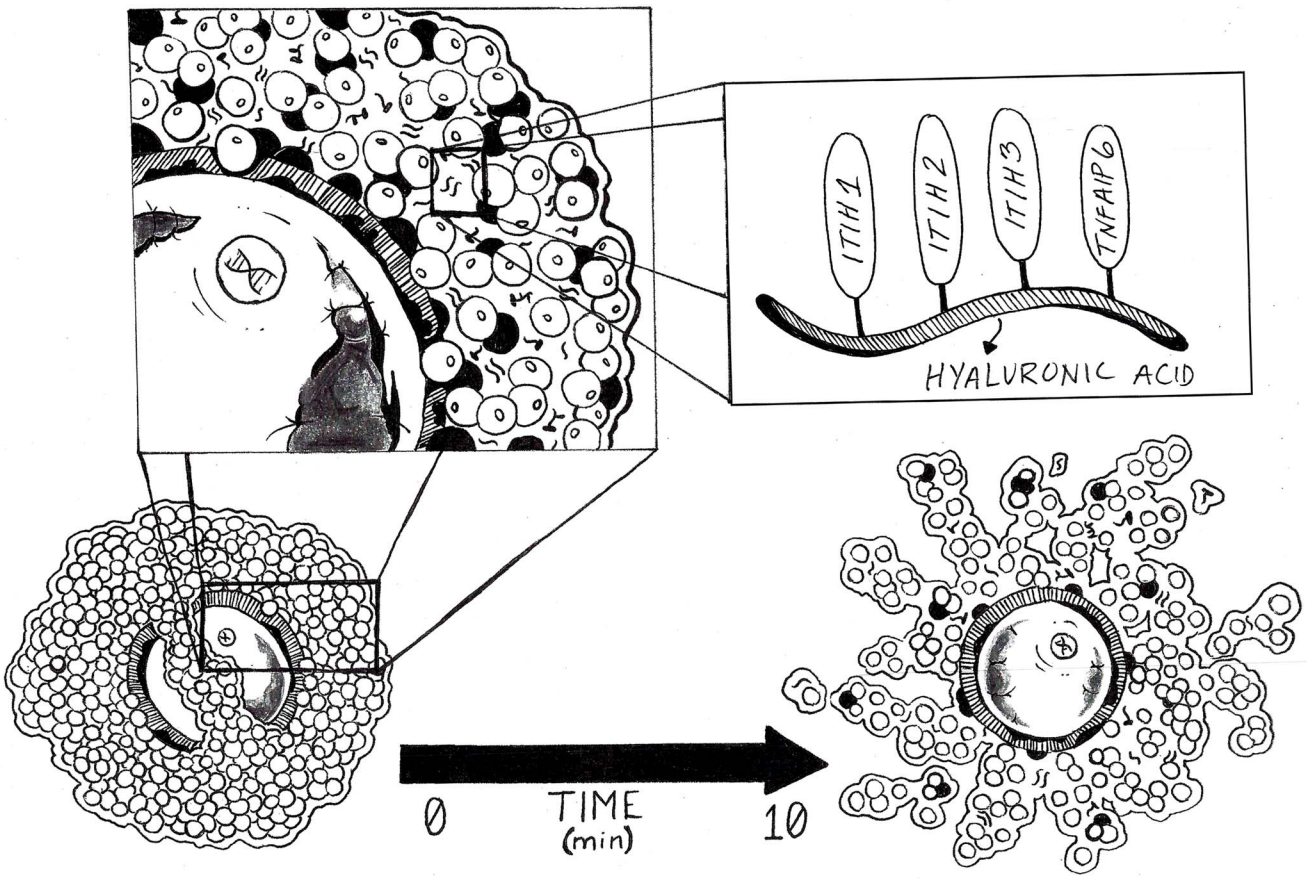


**Key words:** cumulus cells, proteomics, extracellular matrix, hyaluronidase.

## Introduction

Fertilization success depends on a diversity of molecular interactions. Almost ten years ago, reproductive biologists began to appreciate the roles of cumulus cells in fertilization. These cells surround mammalian oocytes and can induce physiological changes in sperm that make them capable of fertilization [1] and enhance fertility through a variety of mechanisms [2, 3].

Importantly, sperm must penetrate the layer of cumulus cells prior to reaching the ovum. In mice, cumulus cells number in the thousands [4] and form a tightly packed layer glued together by female-derived hyaluronic acid and a variety of proteins and sugar molecules [5–7]. Mouse sperm contain at least two hyaluronidases and multiple proteases that are released upon contact with cumulus cells, dissociating them to expose a path to the ovum [8, 9].

Unfortunately, very little is known of the global proteome of the cumulus-oophorus complexes (COCs), which include both oocytes and cumulus cells. Here, we characterize the global COC proteome through cell fractionation and identify a small set of highly abundant proteins involved in extracellular matrix formation, some of which - ITIH1, ITIH3, and VTN - show signatures of recurrent adaptive evolution. In a second follow-up experiment, we show that female mice raised in the presence of multiple males produced COCs that were smaller and more resistant to dissociation by hyaluronidase, consistent with a previous study that demonstrated such females ovulated oocytes that were more resistant to fertilization [15]. Our combination of proteomic, evolutionary, and experimental studies suggest that a subset of the COC proteome may evolve under sexual conflict, whereby cumulus cells slow down fertilization rather than enhance it.

## Materials and methods

All procedures and personnel were approved by the University of Southern California's Institute for Animal Care and Use Committee (protocols #11394 and #11777), and the University of Western Australia's Animal Ethics Committee (approval 03/100/1456).

### Cell collection and protein identification

To identify proteins from different cellular compartments, we used a fractionation-based protein extraction method to isolate cytoplasmic, nuclear, and membrane associated proteins from COCs. Female mice (strain = FVB/NJ) were induced to ovulate as previously described [137, 15, 133]. We used FVB/NJ in order to collect multiple COCs from genetically identical females. Briefly, we injected female mice with 5 IU pregnant mare serum gonadotropin (PMSG) followed 48 hours later with 5 IU human chorionic gonadotropin (hCG).

Twelve hours after hCG injection, we dissected COCs into 1 mL of PBS. We snap-froze COCs in an empty microcentrifuge tube. It is possible that artificial induction of ovulation shifts the COC proteome compared to natural ovulation, but we required large amounts of cells at a single collection time. For this fractionation experiment, entire COCS were homogenized, without separation of cumulus cells from oocytes.

Fractionation and mass spectrometry were performed by ITSI Biosciences, using their ProFEK kit. Samples were reduced using 5 mM TCEP and alkylated using 55 nM iodoacetamide, cleaned with a ToPREP kit, and desalted with the ZipTip kit. Desalted fractions were dried and resuspended in 2% acetonitrile/0.1% formic acid, then loaded onto a Thermo Surveyor HPLC system. Peptides were eluted from the column using a linear acetonitrile gradient from 2 to 30% acetonitrile over 120 minutes followed by high and low organic washes for another 20 minutes, into an LTQ XL mass spectrometer (Thermo Scientific) via a nanospray source with voltage 1.8 V at 180°. A data-dependent Top 5 method was used where a full MS scan from *m/z* 400–1500 was followed by MS/MS scans of the five most abundant ions. Each ion was subjected to collision-induced dissociation. Raw data were searched against the UnitProt *M. musculus* database using Proteome Discoverer 2.2 (Thermo Scientific) and the Sequest HT algorithm.

In a follow-up experiment, we tested the effect of different social environments on COC proteomes, detailed below. To focus on proteins most likely to interact with sperm, we isolated cell surface proteins from cumulus cells after removing oocytes. We collected COCs as above, but then dispersed them using 5 µL of 1 mg/mL hyaluronidase (Sigma, St. Louis MO) and gently swirling the mixture to isolate cumulus cells from oocytes. We used the Pierce Cell Surface Protein Isolation kit (Catalog # 89881, Thermo Fisher Scientific) to biotinylate proteins on the surface of live cumulus cells before lysing them and affinity-purifying the labeled proteins using streptavidin agarose. We concentrated the proteins with a centrifugal 10 K filter, ran them in a single lane of a 12% SDS-PAGE gel at 60 mA for 1 hour to avoid protein separation and cut the single band out for downstream mass spectrometry as described above.

## Comparisons to other datasets

We compared our proteomic data to a previously published microarray transcriptome data generated from mouse COCs [16], submitted to the gene expression omnibus (https://www.ncbi.nlm.nih.gov/geo/) under GSE47967.

In that study, COCs were dissected from mouse ovaries and gene expression of cumulus cells was analyzed from intact COCs (their sample "COC") or after surgically removing the oocytes from COCs (their sample "OOX"). Cells were cultured for 20 hours prior to analysis of gene expression of cumulus cells. We tested whether the genes we identified here were highly expressed in that dataset, relative to the rest of the genome. We quantified gene expression using the Robust Multichip Average method of the Affymetrix Expression Console, as implemented in the LIMMA package in R [17, 18].

Our fractionation experiment aimed to isolate proteins from the cytoplasm, membrane, and nuclear components of COC. We tested whether these cellular components were significantly enriched using Panther GO-SLIM annotations and tools at http://pantherdb.org v.14.0 [19]. For proteins identified in the fractionation experiment, we first assigned proteins to one of these three compartments based on the greatest number of spectra that identified them. Statistical significance ($P < 0.05$) was determined using a Fisher's exact test, with correction for false discovery rate.

## Social manipulation

In a second follow-up experiment, we tested whether female mice produce COCs with unique proteomic characteristics depending on their social environment. A prior study by Firman and Simmons [15] showed that female mice raised in the presence of many males produced COCs that were more resistant to fertilization in vitro, suggesting females can dynamically adjust fertilizability based on their social environment. Following their methodology, we trapped wild house mice from Rat Island off the coast of Western Australia and bred them in facilities at the University of Western Australia for two generations.

At 21 days of age, F2 offspring from six distinct parental pairs were weaned, and full sisters were randomly placed into one of two treatments: (1) females exposed to ten males and thus developing under a "risk" of sperm competition, and (2) females exposed to a single male and thus developing under "no-risk" of sperm competition. In both treatments, females were caged individually. Risk females were positioned next to singly housed sexually mature males. In a separate room, no-risk females were positioned next to singly housed sexually mature females. Risk females received mixed soiled chaff donated from 10 sexually mature males once per week for 8 weeks, while no-risk females received soiled chaff from the same male once every two weeks over the same time period. To control for chaff manipulation, no-risk females received clean chaff on the weeks when they did not receive soiled chaff.

Every two weeks, females of both treatments received supplementary visual, audio, and pheromonal cues. Caged females were placed inside a large plastic tub and encountered a sexually mature individual that had been released into the tub. For 30 minutes, this male roamed freely within the tub and could interact with the female through the wire mesh lid of her cage. Females in the risk treatment encountered a different male each time, while no-risk females only encountered another female. These exposures were aimed at introducing a more tactile cue by which females may perceive a different number of males in the population complementary to receiving soiled chaff. In total, we generated 12 risk and 12 no-risk females. Following 8 weeks of differential male exposure, we induced ovulation as described above, but with 2.5 U PMSG and hCG, collected COCs, and performed proteomics.

## Resistance to hyaluronidase

Sperm must pass through the cumulus cells to reach the egg, and they contain two different hyaluronidases that disperse the cells. Consequently, the density and cohesion of cumulus cells could be a mechanism that accounts for plasticity in ovum fertilizability [15]. For COCs collected from the social manipulation experiment, we monitored the rate at which COCs dispersed upon exposure to hyaluronidase prior to proteomic investigations. We considered the rate of dispersion to be a proxy for COC resistance to hyaluronidase. Although we did not directly test the fertilizability of the COCs collected here, we note that Firman and Simmons [15] previously demonstrated risk females produced eggs that were more resistant to fertilization, using the same social manipulation design. We placed dissected COCs into 1 mL of PBS and added 5 µL of 1 mg/mL hyaluronidase, then obtained an image every 5 seconds for 5 minutes. Using the magnetic lasso tool in Adobe Photoshop CC 2019, we traced the area occupied by cumulus cells. All images were analyzed

blind to treatment. In a few cases, COCs drifted partially out of view during the time-lapse imaging, so we manually estimated the proportion off-screen to adjust the measurements, again done blind to treatment. As cumulus cells dissociate, the 2D area they occupy under a microscope expands. We wrote custom scripts in R version 3.5.1 [18] to analyze the rate of expansion as a proxy for resistance to hyaluronidase. In general, the area of a cumulus mass increased linearly then reached an asymptote after all cells were dissociated, usually within a minute of adding hyaluronidase. We estimated the rate of area increase during this first minute as the slope of a linear model of cumulus area as a function of time, using the model lm(area ~ time). Then, we tested whether these slopes varied by treatment using a weighted *t* test.

### Evolutionary analyses

Proteins involved in fertilization outcomes often undergo recurrent positive selection [20]. To identify COC proteins that are evolving under recurrent positive selection, we performed three different evolutionary comparisons, employing identical methods but for different sets of species. First, we identified one-to-one orthologs shared across seven species, using the Biomart tool of Ensembl version 96 [21]. The seven species included rabbit (*Oryctolagus cuniculus*) build OryCun2.0, thirteen-lined ground squirrel (*Ictidomys tridecemlineatus*) build SpeTri2.0, guinea pig (*Cavia porcellus*) build Cavpor3.0, kangaroo rat (*Dipodomys ordii*) Dord_2.0, rat (*Rattus norvegicus*) build Rnor_6.0, mouse (*Mus musculus*) build GRCm38.p6, and Chinese hamster (*Cricetulus griseus*) build CHOK1GS_Hdv1. We used the phylogenetic tree of Upham et al. [22]. Of 711 proteins identified across all eight of our proteomic experiments described above, 329 had one-to-one orthologs across all seven species.

Second, we repeated the above analysis after excluding kangaroo rat. Upon further inspection, we were concerned about the incomplete sequence data in this reference genome. Of 711 COC proteins identified in the fractionation experiment, 365 had one-to-one orthologs across all six species.

For both the seven-species and the six-species analyses, we downloaded protein and coding sequences from Ensembl version 96, aligned proteins using MUSCLE [23, 24], then associated aligned proteins to their coding sequences using RevTrans [25]. For genes with multiple isoforms, we chose the longest transcript. Genes with fewer than 100 codons present across all species in the alignment were excluded. Then, we fit the M7, M8, and M8a models of evolution [26, 27] using the CODEML tool in PAML software version 4.9 [28]. The M7 model estimates the ratio of nonsynonymous to synonymous divergence ($d_N/d_S$) across codons, with the distribution of $d_N/d_S$ fit to a beta distribution with the constraint that no $d_N/d_S$ class above 1 is allowed. The M8 model relaxes this constraint and estimates an additional $d_N/d_S$ class, as well as a proportion of codons assigned to that class. Twice the difference in log-likelihoods of M7 vs. M8 was tested against a $X^2$ distribution with degrees of freedom equal to the difference in the number of parameters of the two nested models (likelihood ratio test), in this case $df = 2$. To test if the additional $d_N/d_S$ class estimated by the M8 model was significantly greater than 1 (an indication of recurrent positive selection), we compared M8 to the M8a model, which simply fixes the additional class of $d_N/d_S = 1$. We compared the M8 to M8a models using a likelihood ratio test with $df = 1$. Elevated $d_N/d_S$ is an indication that nonsynonymous mutations—assumed to have more functional impact than synonymous mutations—sweep through species more often than neutral expectations.

In a third analysis, we focused on a shallower evolutionary timescale, using 11 mouse species (*Mus platythrix, M. pahari, M. minutoides, M. caroli, M. cervicolor, M. cookii, M. spretus, M. spicilegus, M. macedonicus, M. m. musculus, and M. m. domesticus*), taken from a set of "pseudoreference" sequences generated by Sarver et al. [29]. Briefly, that study used an iterative mapping approach to insert species-specific variants into the C57BL/6 J reference genome. In the construction of pseudoreferences, some sites will not be covered for a particular species, either because those sites are missing (e.g., due to insertion–deletion events) or due to experimental noise (e.g., sequencing efficiency and accuracy). Any sites that were not covered by at least one species were masked in all species and excluded from all downstream analyses. This approach retains the genomic coordinates of the C57BL/6 J reference genome, thus facilitating downstream analyses that rely on annotation. Phylogenetic relationships and branch lengths were taken from Sarver et al. [29].

Following Dean et al. [30], we considered a gene adaptively evolving if (1) the M8 model fit the data better than M7 at $P < 0.05$, where *P*-values were adjusted for multiple comparisons using the Benjamini–Hochberg approach [31], (2) the M8a model fit the data better than M8 at $P < 0.05$, where *P*-values were adjusted for multiple comparisons using the Benjamini–Hochberg approach [31], and (3) at least three codons occurred in this additional class of $d_N/d_S$. Specific codons experiencing recurrent positive selection were those identified with Bayes Empirical Bayes probability >0.9 [32].

## Results

### 711 proteins identified from COCs, with high spectral counts generated from seven proteins involved in the formation and stabilization of extracellular matrix

Across all proteomic experiments, we mapped 24,030 spectra to 711 proteins (Table S1). We mapped each protein with a mean (median) of 33.8 (10) spectra. Eight of these were keratins and were excluded from downstream analyses since they are likely to represent contamination.

The number of spectra generated per protein was very skewed. Inter-alpha trypsin inhibitor, heavy chain 1 (ITIH1) was the protein identified with the most spectra (identified with 1,368 spectra), with more than twice as many spectra as the second highest (ITIH3, identified with 683 spectra) (Table S1). Because these two proteins play important roles in the formation and stabilization of extracellular matrix [33], we investigated in more detail five additional proteins found in extracellular matrix: ITIH2, pentraxin-related gene (PTX3), tumor necrosis factor alpha-induced protein 6 (TNFAIP6), versican (VCAN), and vitronectin (VTN). Together, these seven proteins accounted for over 13% of all spectra generated. However, it should be noted that we did not detect two other extracellular proteins—bikunin (a protein derived from *Ambp*) and aggrecan (ACAN)—known to be present in COC.

In the social manipulation experiment, we only identified 17 proteins from no-risk females and 18 from risk females, 12 of which were present in both groups (Table S1). The number of proteins identified was much smaller than expected, which is probably due to unexpectedly small yield of COC following artificial induction of ovulation in these relatively older and wild-derived animals, as well as the dispersal of cumulus cells during the hyaluronidase resistance experiments.

**Table 1.** Gene ontology analyses of cellular compartment. Columns are the major cellular components targeted in our study (annotated GO term in parentheses). Rows indicate the three compartments of the fractionation experiment, plus our attempt to isolate membrane proteins from the social experiment (number of genes identified in each proteomic experiment in parentheses). Numbers in cells indicate number of proteins identified from particular fractions, which are annotated with that particular GO term. + or − indicate statistically significant enrichment or paucity, respectively.

| Proteome fraction | Membrane (GO:0016020) | Nucleus (GO:0005634) | Cytoplasm (GO:0005737) | Cytosol (GO:0005829) | Extracellular region (GO:0005576) | Extracellular matrix (GO:0031012) |
|---|---|---|---|---|---|---|
| Membrane fraction ($N$ = 209) | 62 (+) | 0 | 87 (+) | 0 | 0 | 0 |
| Cytosolic fraction ($N$ = 244) | 22 (−) | 0 | 135 (+) | 59 (+) | 0 | 0 |
| Nuclear fraction ($N$ = 225) | 10 (−) | 84 (+) | 100 (+) | 55 (+) | 3 (−) | 0 |
| Social experiment ($N$ = 22) | 0 | 0 | 0 | 0 | 0 | 0 |

## Comparison to other datasets confirms these are likely bonafide COC proteins

From 703 non-keratin genes identified, 650 could be matched to a previously published microarray expression dataset from mouse cumulus cells [16]. Those 650 genes showed significantly higher expression in cumulus cells isolated from both COC (cumulus cells plus oocytes) and OOX (cumulus cells only) [re-analysis of data from 16] (median signal intensities = 8.42 vs. 5.59 [8.67 vs. 5.59] compared to the other 21,073 genes identified among COC [OOX] samples; Wilcoxon rank sum test for both comparisons, $P < 10^{-15}$). In other words, the proteins we identified here were highly expressed in a previous study of COCs, lending support to the hypothesis that we identified bonafide COC proteins. In addition, we identified 42% of the 625 proteins found in a previously published mouse oocyte proteome, which did not include cumulus cells [34].

Our fractionation experiment targeted three main cellular compartments. Proteins from the membrane fraction were significantly enriched for the "membrane" annotation, while none were annotated as "nucleus," or "cytosol" (Table 1). Proteins identified from the cytosolic fraction were significantly enriched for "cytosol," significantly depauperate for "membrane," with none annotated as "nucleus" (Table 1). Proteins identified from the nuclear fraction were significantly enriched for "nucleus," "cytoplasm," and "cytosol," while significantly depauperate for "membrane" (Table 1). In sum, proteins isolated from different fractions matched expected Gene Ontology annotations well.

For the social manipulation experiment, we attempted to isolate cell surface proteins. However, neither "membrane" nor "extracellular region" genes were significantly enriched, which is likely due to the small number of proteins identified in our social manipulation experiment.

## Evolutionary analyses identify several extracellular matrix proteins that evolve under recurrent positive selection

We identified 20 adaptively evolving proteins from at least one of the three sets of species (Tables S2, S3, and S4, respectively). No biological processes or molecular functions were significantly enriched among the 20 adaptively evolving genes, using either the whole genome as background or the 703 COC proteins as background. However, several interesting annotations emerged upon manual inspection. Three adaptively evolving genes were related to extracellular matrix formation and stabilization (*Itih1*, *Itih3*, *Vtn*), three had immunity function (*Dhx9*, *Vtn*, *Zp3*), eight were related to regulation of transcription or translation (*Dhx9*, *Dnmt1*, *Hnrnpd*, *Itga2*, *Prpf19*, *Psmc3*, *Syncrip*, *Ybx1*), and four play some role in gamete biology (*Apoa1*, *Pebp1*, *Prdx1*, and *Vtn*). Several genes appeared in more than one of these functional categories.

As pointed out above, a subset of seven proteins that help form and stabilize the extracellular matrix yielded particularly high spectral counts, suggesting they are abundant. Three of these seven (ITIH1, ITIH3, and VTN) have experienced recurrent positive selection (Table S1). For ITIH1, we identified a single codon as positively selected in both the 6-species and 7-species alignments. This codon falls five residues distal to a known proteolytic cleavage site [35], and 22 residues proximal to the Asp residue that covalently bonds to hyaluronic acid [33, 36] (Figure 1). In the *Mus*-only alignment, ten codons were identified as positively selected; these were more dispersed throughout the protein but include a site just eight amino acids proximal to this same proteolytic site (Figure 1).

For ITIH3, we identified six codons experiencing recurrent positive selection from the 6-species and 7-species alignments. Three of these positively selected codons fell within the Von Willebrand factor type A domain (VWA) annotated from this protein (domain #PF00092 from Pfam database version 33.1), a fourth fell within the Inter-alpha-trypsin inhibitor heavy chain C-terminus (ITI_HC_C, #PF06668), and the remaining two fell in a region between the VWA and the same proteolytic site discussed for ITIH1 above (Figure 1). The *Mus*-only alignment did not identify recurrent positive selection for ITIH3. It is interesting to note that a third protein in the ITIH family, ITIH2, barely missed the cutoff for statistical significance, with model M8 fitting the data better than M7 at near significance (uncorrected $P = 0.07$). There was a single codon identified as potentially positively selected, which occurred distal to the proteolytic site mentioned above (Figure 1).

For the extracellular protein VTN, we identified 12 codons under recurrent positive selection across the 6-species, 7-species, and *Mus*-only alignments. Two fell within a hemopexin domain (PF00045), but the rest do not fall within any annotated domains from this protein or known proteolytic cleavage sties [37]. These codons tend to fall within the proximal third of the protein, somewhat close the tripeptide Arg-Gly-Asp (RGD), which is the site that binds to the VWF of ITIH1 and ITIH2 [38], but the potential functional impact of this divergence is unclear.

## Risk females produced COCs that were smaller and more resistant to hyaluronidase

Under ideal conditions, two large COCs can be isolated from a single female, one from each oviduct. However, these often split up into smaller clusters during dissection. Therefore, we analyzed rates of dissociation with a one-tailed weighted *t*-test, where exposure

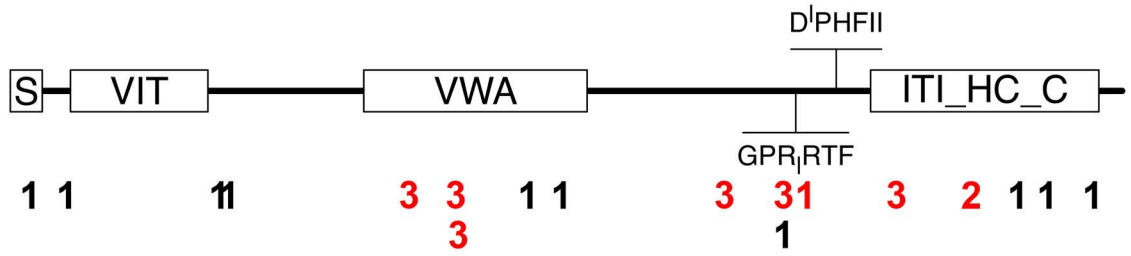


**Figure 1.** General structure of the ITIH proteins. Four boxes indicate four annotated domains that all three ITIH proteins identified here contain: S = signal peptide, VIT = vault protein inter-alpha-trypsin domain (#PF08487), VWA = Von Willebrand factor type A domain (#PF00092), ITI_HC_C = inter-alpha-trypsin inhibitor heavy chain C-terminus (#PF06668). Two additional sequences are highlighted: DPHFII = six amino acid motif that all three ITIH proteins contain. The superscripted character indicates a post-translational cleavage site that exposes the D residue that eventually becomes covalently linked to either chondroitin sulfate or hyaluronic acid (as described in the Discussion). GPRRTF = six amino acid motif present only in ITIH1; the subscripted character indicates the cut site of thrombin [see ref 35]. Numbers below gene model indicate codons identified as experiencing recurrent positive selection for each of the three ITIH proteins (1 = ITIH1, 2 = ITIH2, 3 = ITIH3). Red numbers result from 6-species or 7-species alignments, black numbers result from Mus-only alignments.

treatment (risk vs. no-risk) was the main effect and each cumulus mass was down-weighted by the number of clusters collected per female. COC clusters from risk females dissociated significantly more slowly than those from no-risk females (Figure 2), as measured by the rate of area expansion in the first minute following addition of hyaluronidase (weighted $t = 3.70$, $df = 2.31$, $P = 0.001$; Figure 3). This result held if we performed a non-parametric Wilcoxon rank sum test ($P < 0.001$) instead of a weighted $t$-test.

We also tested whether the initial area of the COCs (normalized by the number of ova in each COC) differed. COC from risk females had significantly smaller initial area compared to no-risk females (weighted $t = 4.43$, $df = 2.41$, $P = 0.0001$; Figure 4). As a consequence, the rate of area expansion in COC clusters from risk females might be underestimated (in the trivial case of a COC with no cumulus cells, we would estimate a rate of expansion close to zero). Upon further examination, the maximum amount of area expansion from risk cumulus clusters was approximately 150% of the starting area (Figure S1), while ten cumulus clusters from no-risk females expanded beyond 150%. We therefore repeated the analysis after excluding all cumulus clusters that expanded more than 150%, which produced qualitatively identical results (weighted $t = 1.76$, $df = 12.50$ $P = 0.05$). Therefore, we conclude that COCs from risk females were both smaller in initial size and were more resistant to hyaluronidase compared to than COCs from no-risk females. In sum, our proteomic and evolutionary analyses above point to the extracellular matrix as a potential influence on fertilization outcomes, while our social manipulation experiment suggests this matrix can be dynamically adjusted based on the environment of an individual female.

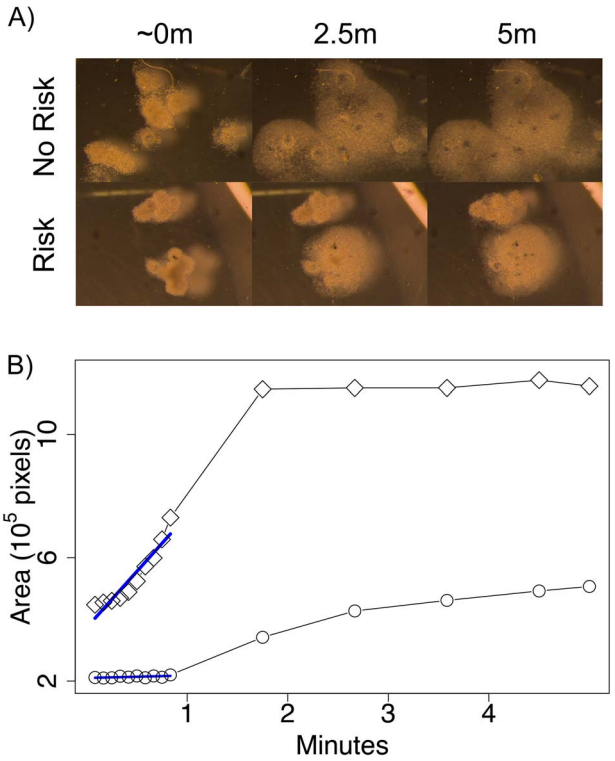


**Figure 2.** (A) After adding hyaluronidase, tightly packed COC begin to dissociate. The three columns contain images of COCs ~0, 2.5, or 5 minutes after exposure to hyaluronidase. The two rows show a characteristic COC from no-risk vs. risk females (specimens NR3_F3 and R3_F7, respectively). The COC from the risk female expanded more slowly; notice the dense cluster of cumulus cells that remain even after 2.5 minutes. In contrast, the no-risk COC was fully dissociated by this time and the eggs clearly visible. (B). We estimated the rate at which COC dissociate by fitting a line through the first 1 minute's worth of areas measured after adding hyaluronidase (blue line). The two line plots are the same two specimens as in A, no-risk female represented by diamonds, risk female represented by circles.

## Discussion

Cumulus cells perform a number of important functions, including the formation of gap junctions, the transfer of nutrients and hormonal signals to oocytes [39, 40], and the alteration of sperm physiology [1, 41–56]. Generally, these functions are described as promoters of fertilization [1, 2, 57–59]. Through a combination of proteomic, evolutionary, and experimental analyses, we present a complementary hypothesis, that a subset of COC proteins involved in the formation and stabilization of extracellular matrix may have evolved as a mechanism for females to modulate (i.e., slow down) fertilization outcomes.

Our hypothesis stems from three main insights. First, seven proteins known to play critical roles in the formation and stabilization of extracellular matrix (ITIH1, ITIH2, ITIH3, PTX3, TNFAIP6, VCAN, and VTN) together accounted for more than 13% of all spectra generated from a total of 711 proteins, suggesting a large component of the COC proteome acts to control access to eggs.

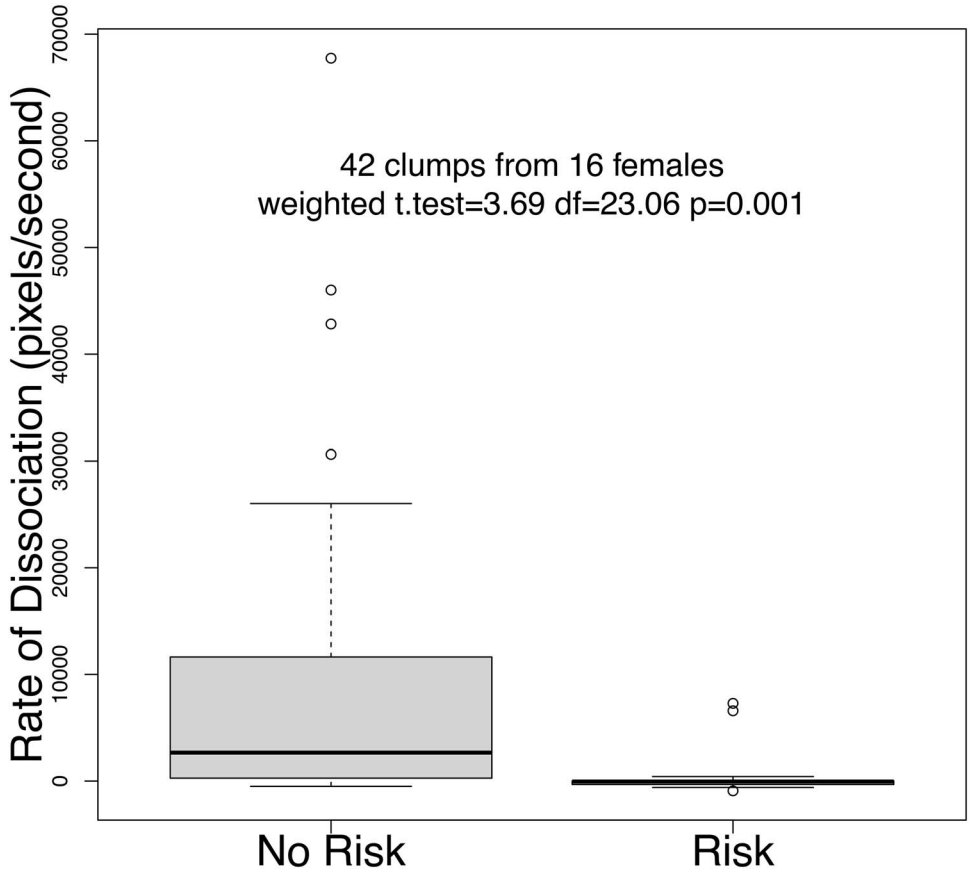


**Figure 3.** COC of no-risk females dissociate more rapidly than risk females.

Second, three of these proteins (ITIH1, ITIH3, and VTN) showed evidence of recurrent positive selection (with ITIH2 just missing our statistical cutoff), a common signature among proteins that influence fertilization rates. Codons experiencing recurrent positive selection tended to fall near functionally important sites, as discussed further below. Third, our social manipulation experiment demonstrated that Risk females produced COCs that were smaller and more resistant to hyaluronidase, offering a possible mechanism for previous observation that females can adjust their ovum fertilizability [15].

## The extracellular matrix of COC

An extracellular matrix enmeshes mammalian COC, acting like a glue to tightly pack cumulus cells around the egg. The main component of this extracellular matrix is hyaluronic acid, produced by cumulus cells [5, 7, 60, 61] in combination with serum-derived factors that prevent the hyaluronic acid from "leaking" out of the COC [7, 62]. We detected seven of these factors—ITIH1, ITIH2, ITIH3, PTX3, TNFAIP6, VCAN, and VTN—at high spectral counts, but did not detect two others—bikunin, a protein derived from *Ambp*, and ACAN known to be present in extracellular matrix.

The three ITIH proteins were the top three (of 711 proteins) in terms of spectral counts identified, suggesting they are abundant. All three ITIH proteins are post-translationally cleaved after the aspartic acid residue in a DPHFII sequence that is identical across all three proteins (Figure 1). This exposes the aspartic acid residue, which becomes covalently bound to hyaluronic acid via three related molecular processes [33, 63, 64]. First, inter-$\alpha$-inhibitor (I$\alpha$I), a complex of the three proteins—bikunin, ITIH1, and ITIH2 all covalently bound to a single chondroitin sulfate chain—enters newly ruptured follicles and associates with the COC extracellular matrix [65–75]. ITIH1 and ITIH2 can remain associated with I$\alpha$I, but the protein TNFAIP6 also acts to transfer the ITIH1 and ITIH2 proteins from the chondroitin sulfate chain of I$\alpha$I to covalently bind directly to hyaluronic acid [75–82]. Second, pre-$\alpha$-inhibitor (P$\alpha$I), a complex of two proteins—bikunin and ITIH3 covalently bound to a single chondroitin sulfate chain—undergoes a very similar process to covalently bind ITIH3 to hyaluronic acid [67, 70, 74, 75, 83, 84]. Third, TNFAIP6 covalently binds to hyaluronic acid and multiple TNFAIP6 are held together via PTX3. All three processes have the effect of stabilizing hyaluronic acid [33], and various knockout experiments in mice have demonstrated these proteins are essential for normal ovulation, COC formation, and fertility [85–90]. VCAN also covalently binds to hyaluronic acid and ITIH1, and VTN binds to ITIH proteins [36, 91], although their effect on the stabilization of extracellular matrix is not well understood.

## Does the extracellular matrix of COC play a role in sexual conflict over fertilization rate?

Sexual reproduction almost always includes some level of conflict between males and females [92]. All else being equal, selection favors males that fertilize more quickly, especially given that females of most species mate with more than one male in a single reproductive cycle (including mice: [93, 94]). However, faster fertilization can be deleterious for females if it inhibits cryptic female choice and/or

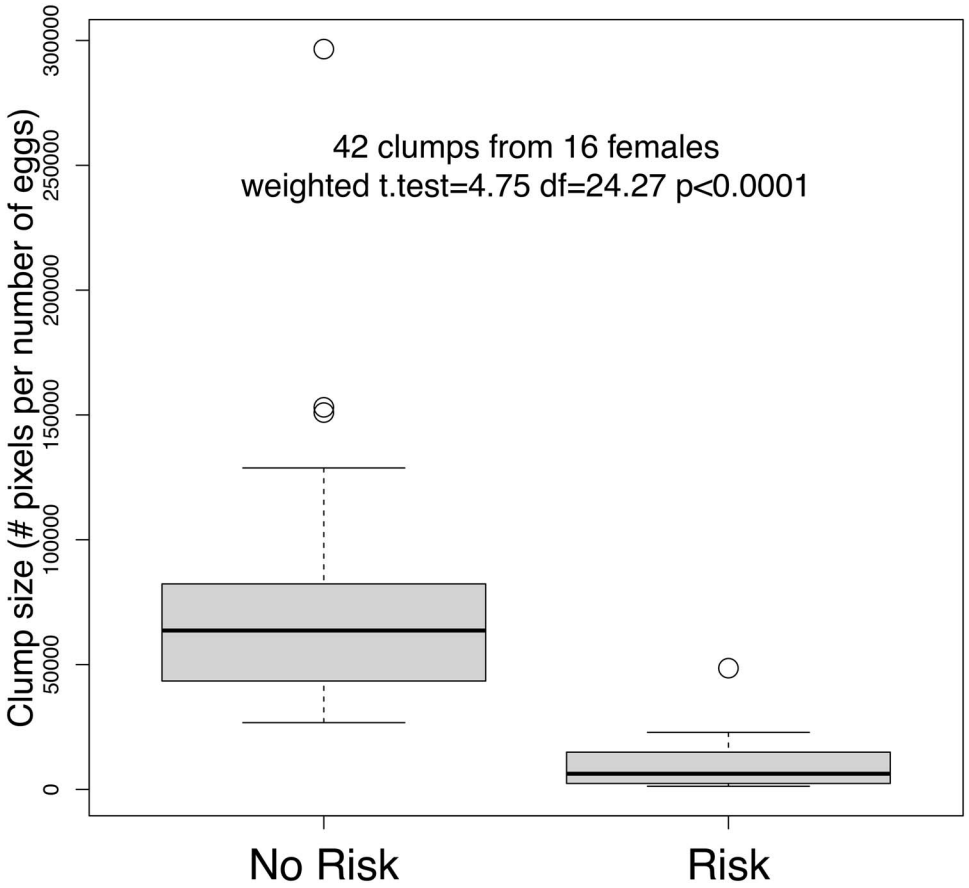


**Figure 4.** The COC from no-risk females were larger at time = 0 minutes than risk females, probably because no-risk COC had more cumulus cells per oocyte (see text).

increases the likelihood of fertilization by more than one sperm, which is lethal in mammals [95, 96]. Therefore, selection is expected to favor females that slow down or otherwise control fertilization [92, 97], resulting in sexual conflict over the rate of fertilization [92, 98].

Consistent with a model of sexual conflict, proteins involved in direct sperm–egg interactions have been shown to undergo recurrent adaptive evolution. Many sperm, seminal fluid, and egg coat proteins have been shown to undergo recurrent positive selection [9, 20, 27, 30, 99–123], which is often concentrated in the actual functional domains that influence sperm-egg binding [99, 100, 118, 123]. In short, sexual conflict appears to fuel a coevolutionary arms race between male and female fertilization proteins across many different species, often described as an interaction between male offenses and female defenses [20, 98]. This signature can be used to generate hypotheses about which sites have functional impact.

Three of seven extracellular proteins involved in stabilization of extracellular matrix (ITIH1, ITIH3, and VTN) showed a significant signature of recurrent positive selection, with a fourth (ITIH2) just missing our statistical cutoff. As discussed above, all three ITIH proteins covalently bind to hyaluronic acid, through esterification of a C-terminal aspartic acid residue that is exposed after a post-translational cleavage event (Figure 1). Both ITIH1 and ITIH3 show recurrent adaptive evolution in a region just upstream of this aspartic acid residue, around a site known to be susceptible to cleavage by thrombin (Figure 1). If these changes alter cleavage patterns in this area, they could influence the rate at which ITIH is effectively removed from their covalent bond to hyaluronic acid, potentially compromising the integrity of the extracellular matrix [35, 36].

These patterns lead to the hypothesis that ITIH proteins modulate fertilization outcomes indirectly by stabilizing the extracellular matrix and creating an obstacle for sperm. In this context, it is interesting that COC proteins playing a more "supportive" role in transferring ITIH proteins to hyaluronic acid, or which are simply less abundant than ITIH proteins (for example, PTX3 and TNFAIP6) do not show evidence of recurrent positive selection. Instead, only the ITIH proteins, which appear to be very abundant and remain covalently bound to hyaluronic acid, thus potentially interacting with sperm and their enzymes, evolve rapidly.

If ITIH proteins evolve under a model of sexual conflict, what are the male-derived proteins they are in conflict with? Sperm contain at least two hyaluronidases (HYAL5 and SPAM1), which are released upon contact with COC to degrade the extracellular matrix and expose a path to the egg [8]. Interestingly, these hyaluronidases also evolve under recurrent positive selection [9–12], perhaps reflecting coevolution with female-derived proteins like the ITIH's [13, 14, 124]. Sperm-derived hyaluronidases are not known to directly act on the ITIH proteins, but sperm and seminal fluid also contain a diversity of proteases and protease inhibitors [9, 110, 111] that could feasibly regulate degradation of the extracellular matrix. Many of these also evolve under recurrent positive selection [9, 110, 111]. Interestingly, a critical function of both the IαI and

PαI protein complexes is as a protease inhibitor, consistent with a possible role in resistance of the COC proteome to degradation [33].

It should be noted that many of the proteins discussed here have additional functions that also predict rapid evolution. For example, the ITIH proteins and VTN also participate in immune regulation [34, 36, 125–128], as well as protection from venom [129, 130]. As these proteins circulate in the serum of both males and females, it is not surprising they have additional functions outside of COC development. It is possible that host–pathogen or predator–prey interactions drive at least some portion of the recurrent positive selection observed in these ITIH proteins.

### Risk females produced COC that were smaller and more resistant to hyaluronidase

We also showed that females raised in the presence of multiple males produced COCs, which were smaller and more resistant to hyaluronidase compared to females raised in the presence of a single male. This independent experiment further implicates the extracellular matrix of the COC as a potential modulator of fertilization rate, in this case one that is plastic with respect to an individual's environment [15, 131].

Unfortunately, we did not generate as many spectra as anticipated from the socially manipulation experiment, likely a combination of failed induction of ovulation as well as loss of proteins during experimental exposure to hyaluronidase. For example, we did not detect any of the ITIH proteins or their interacting proteins in the social manipulation experiment. We therefore interpret the proteomic results of this follow-up experiment with caution. Nevertheless, the small number of proteins we detected suggests that risk females reach sexual maturity at an earlier age than no-risk females. We identified ENO1 and PKM only from risk females, both of which correlate with a metabolic shift in the cumulus cells of older, cycling females [132]. Conversely, we identified APOA1 only from no-risk females, which has been associated with females that are yet to reach sexual maturity [132]. Interestingly, artificial induction of ovulation is known to fail more often in females that have already begun natural estrus cycling [133], and roughly 50% of risk females failed to ovulate in our social manipulation experiment. Therefore, even though chronologic age was controlled in our experiment, risk females may have been reproductively older and produced COCs with different biological characteristics compared to no-risk females. These results are consistent with findings that female mice exposed to male urinary proteins and physical interaction with males reach sexual maturity at an earlier age [134, 135]. In sum, it remains unknown how much of the "plasticity" we observe in our social manipulation experiment is due to differences in reproductive ageing across treatments.

## Conclusions

A large body of literature views cumulus cells as enhancers of fertilization. Our study offers an alternative view, that the extracellular matrix of the COC represents an important female-derived obstacle to fertilization. A model of sexual conflict does well to explain these patterns, including our finding that females raised in the presence of multiple males produce COC with a more resistant extracellular matrix.

In the future, it will be important to directly test the interactions between female-derived and male-derived proteins and structures. If sexual conflict drives the evolution of some of these proteins, then fertilization outcomes should depend on the combination of female-derived proteins that form and stabilize the extracellular matrix of COC and the male-derived molecules that presumably break it down. Ample genetic variation for all three ITIH proteins and the two sperm hyaluronidases exists among various strains and species of mice [136], enabling future direct tests of this hypothesis.

## Supplementary Material

Supplementary Material is available at *BIOLRE* online.

## Availability of data and materials

Raw spectral data of all proteomic experiments are archived at the ProteomeXchange repository, DOI:"to be determined." All raw image data, scripts, and summaries of image data of hyaluronidase assays are archived at Dryad, DOI:"to be determined." All data that underlie evolutionary inferences (DNA sequences, protein sequences, alignments) are archived at Dryad, DOI:"to be determined."

## Author contributions

S.K., R.C.F., L.W.S., and M.D.D. conceived and designed the research. S.K. performed the research. B.A.J.S. assisted with phylogenetic inference. N.L.C. performed and analyzed proteomic experiments. S.K. and M.D.D. analyzed data and wrote the paper, with contributions from all authors.

## Acknowledgements

We thank Gonçalo André and Jessica Moran for assistance with mouse husbandry and Stephanie Duran for assistance in image measurements. Ebrahim Zandi (USC) and Stephen Russell (ITSI) assisted with proteomics. Caleb Ghione created the graphical abstract.

**Conflict of Interest**: The authors declare no conflict of interest.

## References

1. Jin M, Fujiwara E, Kakiuchi Y, Okabe M, Satouh Y, Baba SA, Chiba K, Hirohashi N. Most fertilizing mouse spermatozoa begin their acrosome reaction before contact with the zona pellucida during in vitro fertilization. *Proc Natl Acad Sci* 2011; **108**:4892–4896.
2. Tanghe S, Van Soom A, Nauwynck H, Coryn M, de Kruif A. Minireview: Functions of the cumulus oophorus during oocyte maturation, ovulation, and fertilization. *Mol Reprod Dev* 2002; **61**:414–424.
3. Van Soom A, Tanghe S, De Pauw I, Maes D, De Kruif A. Function of the cumulus oophorus before and during mammalian fertilization. *Reprod Domest Anim* 2002; **37**:144–151.
4. Leese HJ, Barton AM. Production of pyruvate by isolated mouse cumulus cells. *J Exp Zool* 1985; **234**:231–236.
5. Eppig JJ. FSH stimulates hyaluronic acid synthesis by oocyte-cumulus cell complexes from mouse preovulatory follicles. *Nature* 1979; **281**:483–484.
6. Ball G, Bellin M, Ax R, First N. Glycosaminoglycans in bovine cumulus-oocyte complexes: Morphology and chemistry. *Mol Cell Endocrinol* 1982; **28**:113–122.
7. Salustri A, Yanagishita M, Hascall VC. Synthesis and accumulation of hyaluronic acid and proteoglycans in the mouse cumulus cell-oocyte

complex during follicle-stimulating hormone-induced mucification. *J Biol Chem* 1989; **264**:13840–13847.
8. Kimura M, Kim E, Kang W, Yamashita M, Saigo M, Yamazaki T, Nakanishi T, Kashiwabara S-I, Baba T. Functional roles of mouse sperm hyaluronidases, HYAL5 and SPAM1, in fertilization1. *Biol Reprod* 2009; **81**:939–947.
9. Dorus S, Wasbrough ER, Busby J, Wilkins EC, Karr TL. Sperm proteomics reveals intensified selection on mouse sperm membrane and acrosome genes. *Mol Biol Evol* 2010; **27**:1235–1246.
10. Gmachl M, Sagan S, Ketter S, Kreil G. The human sperm protein PH-20 has hyaluronidase activity. *FEBS Lett* 1993; **336**:545–548.
11. Lin Y, Mahan K, Lathrop WF, Myles DG, Primakoff P. A hyaluronidase activity of the sperm plasma membrane protein PH-20 enables sperm to penetrate the cumulus cell layer surrounding the egg. *J Cell Biol* 1994; **125**:1157–1163.
12. Prothmann A, Laube I, Dietz J, Roos C, Mengel K, Zischler H, Herlyn H. Sexual size dimorphism predicts rates of sequence evolution of SPerm adhesion molecule 1 (SPAM1, also PH-20) in monkeys, but not in hominoids (apes including humans). *Mol Phylogenet Evol* 2012; **63**:52–63.
13. Moore H, Bedford J. An in vivo analysis of factors influencing the fertilization of hamster eggs. *Biol Reprod* 1978; **19**:879–885.
14. Hunter R. Ovarian control of very low sperm/egg ratios at the commencement of mammalian fertilisation to avoid polyspermy. *Mol Reprod Dev* 1996; **44**:417–422.
15. Firman RC, Simmons LW. Sperm competition risk generates phenotypic plasticity in ovum fertilizability. *Proceedings of the Royal Society B: Biological Sciences* 2013; **280**:20132097.
16. Emori C, Wigglesworth K, Fujii W, Naito K, Eppig JJ, Sugiura K. Cooperative effects of 17$\beta$-estradiol and oocyte-derived paracrine factors on the transcriptome of mouse cumulus cells. *Endocrinology* 2013; **154**:4859–4872.
17. Ritchie ME, Phipson B, Wu D, Hu Y, Law CW, Shi W, Smyth GK. Limma powers differential expression analyses for RNA-sequencing and microarray studies. *Nucleic Acids Res* 2015; **43**:e47–e47.
18. R Core Team. *R: A language and environment for statistical computing*. Vienna, Austria: R Foundation for Statistical Computing; 2014; http://www.R-project.org/.
19. Mi H, Huang X, Muruganujan A, Tang H, Mills C, Kang D, Thomas PD. PANTHER version 11: Expanded annotation data from gene ontology and reactome pathways, and data analysis tool enhancements. *Nucleic Acids Res* 2017; **45**:D183–D189.
20. Clark NL, Aagaard JE, Swanson WJ. Evolution of reproductive proteins from animals and plants. *Reprod Fertil Dev* 2006; **131**:11–22.
21. Hunt SE, McLaren W, Gil L, Thormann A, Schuilenburg H, Sheppard D, Parton A, Armean IM, Trevanion SJ, Flicek P. Ensembl variation resources. *Database* 2018; **2018**:bay119. doi: 10.1093/database/bay119.
22. Upham NS, Esselstyn JA, Jetz W. Inferring the mammal tree: Species-level sets of phylogenies for questions in ecology, evolution, and conservation. *PLoS Biol* 2019; **17**:e3000494.
23. Edgar RC. MUSCLE: Multiple sequence alignment with high accuracy and high throughput. *Nucleic Acids Res* 2004; **32**:1792–1797.
24. Edgar RC. MUSCLE: A multiple sequence alignment method with reduced time and space complexity. *BMC Bioinformatics* 2004; **5**:113.
25. Wernersson R, Pedersen AG. RevTrans: Multiple alignment of coding DNA from aligned amino acid sequences. *Nucleic Acids Res* 2003; **31**:3537–3539.
26. Yang Z, Nielsen R, Goldman N, Pedersen A-MK. Codon-substitution models for heterogeneous selection pressure at amino acid sites. *Genetics* 2000; **155**:431–449.
27. Swanson WJ, Nielsen R, Yang Q. Pervasive adaptive evolution in mammalian fertilization proteins. *Mol Biol Evol* 2003; **20**:18–20.
28. Yang Z. PAML 4: Phylogenetic analysis by maximum likelihood. *Mol Biol Evol* 2007; **24**:1586–1591.
29. Sarver B, Keeble S, Cosart T, Tucker P, Dean MD, Good JM. Phylogenomic insights into mouse evolution using a pseudoreference approach. *Genome Biol Evol* 2017; **9**:726–739.
30. Dean MD, Good JM, Nachman MW. Adaptive evolution of proteins secreted during sperm maturation: An analysis of the mouse epididymal transcriptome. *Mol Biol Evol* 2008; **25**:383–392.
31. Benjamini Y, Hochberg Y. Controlling the false discovery rate: A practical and powerful approach to multiple testing. *J R Stat Soc B Methodol* 1995; **57**:289–300.
32. Yang Z, Wong WS, Nielsen R. Bayes empirical bayes inference of amino acid sites under positive selection. *Mol Biol Evol* 2005; **22**:1107–1118.
33. Russell DL, Salustri A. Extracellular matrix of the cumulus-oocyte complex. *Semin Reprod Med* 2006; **24**:217–227.
34. Zhang P, Ni X, Guo Y, Guo X, Wang Y, Zhou Z, Huo R, Sha J. Proteomic-based identification of maternal proteins in mature mouse oocytes. *BMC Genomics* 2009; **10**:348.
35. Petrey AC, de la Motte CA. Thrombin cleavage of inter-$\alpha$-inhibitor heavy chain 1 regulates leukocyte binding to an inflammatory hyaluronan matrix. *J Biol Chem* 2016; **291**:24324–24334.
36. Briggs DC, Langford-Smith AW, Birchenough HL, Jowitt TA, Kielty CM, Enghild JJ, Baldock C, Milner CM, Day AJ. Inter-$\alpha$-inhibitor heavy chain-1 has an integrin-like 3D structure mediating immune regulatory activities and matrix stabilization during ovulation. *J Biol Chem* 2020; **295**:5278–5291.
37. Schvartz I, Seger D, Shaltiel S. Vitronectin. *Int J Biochem Cell Biol* 1999; **31**:539–544.
38. Adair JE, Stober V, Sobhany M, Zhuo L, Roberts JD, Negishi M, Kimata K, Garantziotis S. Inter-$\alpha$-trypsin inhibitor promotes bronchial epithelial repair after injury through vitronectin binding. *J Biol Chem* 2009; **284**:16922–16930.
39. Eppig JJ. The relationship between cumulus cell-oocyte coupling, oocyte meiotic maturation, and cumulus expansion. *Dev Biol* 1982; **89**:268–272.
40. Eppig JJ. Intercommunication between mammalian oocytes and companion somatic cells. *Bioessays* 1991; **13**:569–574.
41. Austin C, Walton A. Fertilization. In: Parkes A (ed.), *Marshall's Physiology of Reproduction*, vol. **1**. London, England: Longmans Green; 1960: 310–416.
42. Tesarik J, Pilka L, Drahorad J, Cechova D, Veselsky L. The role of cumulus cell-secreted proteins in the development of human sperm fertilizing ability: Implication in IVF. *Hum Reprod* 1988; **3**:129–132.
43. Ito M, Smith T, Yanagimachi R. Effect of ovulation on sperm transport in the hamster oviduct. *J Reprod Fertil* 1991; **93**:157–163.
44. Bedford J, Kim H. Cumulus oophorus as a sperm sequestering device, in vivo. *J Exp Zool A Ecol Genet Physiol* 1993; **265**:321–328.
45. Eisenbach M, Tur-Kaspa I. Do human eggs attract spermatozoa? *Bioessays* 1999; **21**:203–210.
46. Chian R, Park C, Sirard M. Cumulus cells act as a sperm trap during in vitro fertilization of bovine oocytes. *Theriogenology* 1996; **45**:258.
47. Sun F, Bahat A, Gakamsky A, Girsh E, Katz N, Giojalas LC, Tur-Kaspa I, Eisenbach M. Human sperm chemotaxis: Both the oocyte and its surrounding cumulus cells secrete sperm chemoattractants. *Hum Reprod* 2005; **20**:761–767.
48. Ijaz A, Lambert RD, Sirard MA. In vitro-cultured bovine granulosa and oviductal cells secrete sperm motility-maintaining factor (s). *Mol Reprod Dev* 1994; **37**:54–60.
49. Kalthur G, Kumar P, Adiga SK. Enhancement in motility of sperm co-incubated with cumulus oocyte complex (COC) in vitro. *Eur J Obstet Gynecol Reprod Biol* 2009; **145**:167–171.
50. Hong S-J, Chiu PC-N, Lee K-F, Tse JY-M, Ho P-C, Yeung WS-B. Cumulus cells and their extracellular matrix affect the quality of the spermatozoa penetrating the cumulus mass. *Fertil Steril* 2009; **92**: 971–978.
51. Gwatkin R, Andersen O, Hutchinson C. Capacitation of hamster spermatozoa in vitro: The role of cumulus components. *J Reprod Fertil* 1972; **30**:389–394.
52. Carrell DT, Middleton R, Peterson C, Jones K, Urry R. Role of the cumulus in the selection of morphologically normal sperm and induction of the acrosome reaction during human in vitro fertilization. *Arch Androl* 1993; **31**:133–137.

53. Yin L, Chung C, Huo R, Liu H, Zhou C, Xu W, Zhu H, Zhang J, Shi Q, Wong H. A sperm GPI-anchored protein elicits sperm-cumulus cross-talk leading to the acrosome reaction. *Cell Mol Life Sci* 2009; **66**:900–908.
54. Sun TT, Chung CM, Chan HC. Acrosome reaction in the cumulus oophorus revisited: Involvement of a novel sperm-released factor NYD-SP8. *Protein Cell* 2011; **2**:92–98.
55. Bavister BD. Evidence for a role of post-ovulatory cumulus components in supporting fertilizing ability of hamster spermatozoa. *J Androl* 1982; **3**:365–372.
56. Drahorad J, Tesařík J, Čechová D, Vilim V. Proteins and glycosaminoglycans in the intercellular matrix of the human cumulus–oophorus and their effect on conversion of proacrosin to acrosin. *Reproduction* 1991; **93**:253–262.
57. Hong S-J, Tse JY, Ho P-C, Yeung WS-B. Cumulus cells reduce the spermatozoa–zona binding inhibitory activity of human follicular fluid. *Fertil Steril* 2003; **79**:802–807.
58. Tanii I, Aradate T, Matsuda K, Komiya A, Fuse H. PACAP-mediated sperm–cumulus cell interaction promotes fertilization. *Reproduction* 2011; **141**:163–171.
59. Chen H, Kui C, Chan HC. Ca2+ mobilization in cumulus cells: Role in oocyte maturation and acrosome reaction. *Cell Calcium* 2013; **53**:68–75.
60. Chen L, Wert SE, Hendrix EM, Russell PT, Cannon M, Larsen WJ. Hyaluronic acid synthesis and gap junction endocytosis are necessary for normal expansion of the cumulus mass. *Mol Reprod Dev* 1990; **26**:236–247.
61. Salustri A, Yanagishita M, Underhill CB, Laurent TC, Hascall VC. Localization and synthesis of hyaluronic acid in the cumulus cells and mural granulosa cells of the preovulatory follicle. *Dev Biol* 1992; **151**: 541–551.
62. Eppig JJ. Role of serum in FSH stimulated cumulus expansion by mouse oocyte-cumulus cell complexes in vitro. *Biol Reprod* 1980; **22**:629–633.
63. Zhuo L, Hascall VC, Kimata K. Inter-α-trypsin inhibitor, a covalent protein-glycosaminoglycan-protein complex. *J Biol Chem* 2004; **279**:38079–38082.
64. Lord MS, Melrose J, Day AJ, Whitelock JM. The inter-α-trypsin inhibitor family: Versatile molecules in biology and pathology. *J Histochem Cytochem* 2020; **68**:907–927.
65. Nagyova E. Organization of the expanded cumulus-extracellular matrix in preovulatory follicles: A role for inter-alpha-trypsin inhibitor. *Endocr Regul* 2015; **49**:37–45.
66. Briggs DC, Langford-Smith AW, Birchenough HL, Jowitt TA, Kielty CM, Enghild JJ, Baldock C, Milner CM, Day AJ. Inter-α-inhibitor heavy chain-1 has an integrin-like 3D structure mediating immune regulatory activities and matrix stabilization during ovulation. *Journal of Biological Chemistry* 2020; **295**:5278–5291.
67. Bost F, Diarra-Mehrpour M, Martin J-P. Inter-α-trypsin inhibitor proteoglycan family. *Eur J Biochem* 1998; **252**:339–346.
68. Chen L, Mao S, McLean LR, Powers RW, Larsen WJ. Proteins of the inter-alpha-trypsin inhibitor family stabilize the cumulus extracellular matrix through their direct binding with hyaluronic acid. *J Biol Chem* 1994; **269**:28282–28287.
69. Chen L, Mao S, Larsen WJ. Identification of a factor in fetal bovine serum that stabilizes the cumulus extracellular matrix. A role for a member of the inter-alpha-trypsin inhibitor family. *J Biol Chem* 1992; **267**:12380–12386.
70. Enghild JJ, Thøgersen I, Pizzo SV, Salvesen G. Analysis of inter-alpha-trypsin inhibitor and a novel trypsin inhibitor, pre-alpha-trypsin inhibitor, from human plasma. Polypeptide chain stoichiometry and assembly by glycan. *J Biol Chem* 1989; **264**:15975–15981.
71. Kobayashi H, Hirashima Y, Sun GW, Fujie M, Nishida T, Takigawa M, Terao T. Identity of urinary trypsin inhibitor-binding protein to link protein. *J Biol Chem* 2000; **275**:21185–21191.
72. Camaioni A, Hascall VC, Yanagishita M, Salustri A. Effects of exogenous hyaluronic acid and serum on matrix organization and stability in the mouse cumulus cell-oocyte complex. *J Biol Chem* 1993; **268**:20473–20481.
73. Jessen TE, Faarvang KL, Ploug M. Carbohydrate as covalent crosslink in human inter-α-trypsin inhibitor: A novel plasma protein structure. *FEBS Lett* 1988; **230**:195–200.
74. Zhao M, Yoneda M, Ohashi Y, Kurono S, Iwata H, Ohnuki Y, Kimata K. Evidence for the covalent binding of SHAP, heavy chains of inter-α-trypsin inhibitor, to hyaluronan. *J Biol Chem* 1995; **270**:26657–26663.
75. Thogersen IB, Enghild JJ. Biosynthesis of Bikunin proteins in the human carcinoma cell line HepG2 and in primary human hepatocytes polypeptide assembly by glycosaminoglycan. *J Biol Chem* 1995; **270**:18700–18709.
76. Sanggaard KW, Hansen L, Scavenius C, Wisniewski H-G, Kristensen T, Thøgersen IB, Enghild JJ. Evolutionary conservation of heavy chain protein transfer between glycosaminoglycans. *Biochimica et Biophysica Acta (BBA)-Proteins and Proteomics* 2010; **1804**:1011–1019.
77. Briggs DC, Birchenough HL, Ali T, Rugg MS, Waltho JP, Ievoli E, Jowitt TA, Enghild JJ, Richter RP, Salustri A. Metal ion-dependent heavy chain transfer activity of TSG-6 mediates assembly of the cumulus-oocyte matrix. *J Biol Chem* 2015; **290**:28708–28723.
78. Wisniewski H-G, Burgess WH, Oppenheim JD, Vilcek J. TSG-6, an arthritis-associated Hyaluronan binding protein, forms a stable complex with the serum protein inter-alpha inhibitor. *Biochemistry* 1994; **33**:7423–7429.
79. Milner CM, Day AJ. TSG-6: A multifunctional protein associated with inflammation. *J Cell Sci* 2003; **116**:1863–1873.
80. Mukhopadhyay D, Hascall VC, Day AJ, Salustri A, Fülöp C. Two distinct populations of tumor necrosis factor-stimulated gene-6 protein in the extracellular matrix of expanded mouse cumulus cell–oocyte complexes. *Arch Biochem Biophys* 2001; **394**:173–181.
81. Huang L, Yoneda M, Kimata K. A serum-derived hyaluronan-associated protein (SHAP) is the heavy chain of the inter alpha-trypsin inhibitor. *J Biol Chem* 1993; **268**:26725–26730.
82. Rugg MS, Willis AC, Mukhopadhyay D, Hascall VC, Fries E, Fülöp C, Milner CM, Day AJ. Characterization of complexes formed between TSG-6 and inter-α-inhibitor that act as intermediates in the covalent transfer of heavy chains onto hyaluronan. *J Biol Chem* 2005; **280**:25674–25686.
83. Kaczmarczyk A, Thuveson M, Fries E. Intracellular coupling of the heavy chain of pre-α-inhibitor to chondroitin sulfate. *J Biol Chem* 2002; **277**:13578–13582.
84. Enghild JJ, Salvesen G, Hefta S, Thøgersen I, Rutherfurd S, Pizzo S. Chondroitin 4-sulfate covalently cross-links the chains of the human blood protein pre-alpha-inhibitor. *J Biol Chem* 1991; **266**: 747–751.
85. Sato H, Kajikawa S, Kuroda S, Horisawa Y, Nakamura N, Kaga N, Kakinuma C, Kato K, Morishita H, Niwa H. Impaired fertility in female mice lacking urinary trypsin inhibitor. *Biochem Biophys Res Commun* 2001; **281**:1154–1160.
86. Zhuo L, Yoneda M, Zhao M, Yingsung W, Yoshida N, Kitagawa Y, Kawamura K, Suzuki T, Kimata K. Defect in SHAP-hyaluronan complex causes severe female infertility; a study by inactivation of the *bikunin* gene in mice. *J Biol Chem* 2001; **276**:7693–7696.
87. Suzuki M, Kobayashi H, Tanaka Y, Kanayama N, Terao T. Reproductive failure in mice lacking inter-alpha-trypsin inhibitor (ITI)–ITI target genes in mouse ovary identified by microarray analysis. *J Endocrinol* 2004; **183**:29–38.
88. Fülöp C, Szántó S, Mukhopadhyay D, Bárdos T, Kamath RV, Rugg MS, Day AJ, Salustri A, Hascall VC, Glant TT. Impaired cumulus mucification and female sterility in tumor necrosis factor-induced protein-6 deficient mice. *Development* 2003; **130**:2253–2261.
89. Salustri A, Garlanda C, Hirsch E, De Acetis M, Maccagno A, Bottazzi B, Doni A, Bastone A, Mantovani G, Peccoz PB. PTX3 plays a key role in the organization of the cumulus oophorus extracellular matrix and in in vivo fertilization. *Development* 2004; **131**:1577–1586.
90. Varani S, Elvin JA, Yan C, DeMayo J, DeMayo FJ, Horton HF, Byrne MC, Matzuk MM. Knockout of pentraxin 3, a downstream target of growth differentiation factor-9, causes female subfertility. *Mol Endocrinol* 2002; **16**:1154–1167.

91. Russell DL, Ochsner SA, Hsieh M, Mulders S, Richards JS. Hormone-regulated expression and localization of versican in the rodent ovary. *Endocrinology* 2003; **144**:1020–1031.
92. Arnqvist G, Rowe L. *Sexual conflict*. Princeton, New Jersey: Princeton University Press; 2005.
93. Dean MD, Ardlie KG, Nachman MW. The frequency of multiple paternity suggests that sperm competition is common in house mice (*Mus domesticus*). *Mol Ecol* 2006; **15**:4141–4151.
94. Firman RC, Simmons LW. The frequency of multiple paternity predicts variation in testes size among island populations of house mice. *J Evol Biol* 2008; **21**:1524–1533.
95. Austin CR, Braden AW. Polyspermy in mammals. *Nature* 1953; **172**:82–83.
96. Fraser LR, Maudlin I. Relationship between sperm concentration and the incidence of polyspermy in mouse embryos fertilized in vitro. *J Reprod Fertil* 1978; **52**:103–106.
97. Frank SA. Sperm competition and female avoidance of polyspermy mediated by sperm–egg biochemistry. *Evolutionary Ecology Research* 2000; **2**:613–625.
98. Firman RC. Postmating sexual conflict and female control over fertilization during gamete interaction. *Ann N Y Acad Sci* 2018; **1422**:48–64.
99. Gasper J, Swanson WJ. Molecular population genetics of the gene encoding the human fertilization protein *zonadhesin* reveals rapid adaptive evolution. *The American Journal of Human Genetics* 2006; **79**:820–830.
100. Grayson P, Civetta A. Positive selection in the adhesion domain of Mus sperm Adam genes through gene duplications and function-driven gene complex formations. *BMC Evol Biol* 2013; **13**:217.
101. Grayson P, Civetta A. Positive selection and the evolution of *izumo* genes in mammals. *International Journal of Evolutionary Biology* 2012; **2012**:7.
102. Swanson WJ, Clark AG, Waldrip-Dail HM, Wolfner MF, Aquadro CF. Evolutionary EST analysis identifies rapidly evolving male reproductive proteins in *Drosophila*. *Proc Natl Acad Sci U S A* 2001; **98**:7375–7379.
103. Swanson WJ, Vacquier VD. The rapid evolution of reproductive proteins. *Nat Rev Genet* 2002; **3**:137–144.
104. Vacquier VD, Swanson WJ. Selection in the rapid evolution of gamete recognition proteins in marine invertebrates. *Cold Spring Harb Perspect Biol* 2011; **3**:a002931.
105. Dapper AL, Wade MJ. The evolution of sperm competition genes: The effect of mating system on levels of genetic variation within and between species. *Evolution* 2016n/a-n/a; **70**:502–511.
106. Wilburn DB, Swanson WJ. From molecules to mating: Rapid evolution and biochemical studies of reproductive proteins. *J Proteomics* 2016; **135**:12–25.
107. Tsaur SC, Wu CI. Positive selection and the molecular evolution of a gene of male reproduction, *Acp26Aa* of *Drosophila*. *Mol Biol Evol* 1997; **14**:544–549.
108. Aguadé M. Positive selection drives the evolution of the Acp29AB accessory gland protein in drosophila. *Genetics* 1999; **152**:543–551.
109. Wolfner MF. The gifts that keep on giving: Physiological functions and evolutionary dynamics of male seminal proteins in drosophila. *Heredity* 2002; **88**:85–93.
110. Dean MD, Clark NL, Findlay GD, Karn RC, Yi X, Swanson WJ, MacCoss MJ, Nachman MW. Proteomics and comparative genomic investigations reveal heterogeneity in evolutionary rate of male reproductive proteins in mice (*Mus domesticus*). *Mol Biol Evol* 2009; **26**:1733–1743.
111. Dean MD, Findlay GD, Hoopmann MR, Wu CC, MacCoss MJ, Swanson WJ, Nachman MW. Identification of ejaculated proteins in the house mouse (*Mus domesticus*) via isotopic labeling. *BMC Genomics* 2011; **12**:306.
112. Clark NL, Gasper J, Sekino M, Springer SA, Aquadro CF, Swanson WJ. Coevolution of interacting fertilization proteins. *PLoS Genet* 2009; **5**:e1000570.
113. Clark NL, Swanson WJ. Pervasive adaptive evolution in primate seminal proteins. *PLoS Genet* 2005; **1**:e35.
114. Swanson WJ, Yang Z, Wolfner MF, Aquadro CF. Positive Darwinian selection drives the evolution of several female reproductive proteins in mammals. *Proc Natl Acad Sci U S A* 2001; **98**:2509–2514.
115. Galindo BE, Vacquier VD, Swanson WJ. Positive selection in the egg receptor for abalone sperm lysin. *Proc Natl Acad Sci U S A* 2003; **100**:4639–4643.
116. Todd SC, Levy S, Mayrhofer G, Ashman LK, Koyama M, Yamaoko M, Sasada R, Radford KJ, Mallesch J, Hersey P, Mannion BA, Berditchevski F et al. Requirement of CD9 on the egg plasma membrane for fertilization. *Science* 2000; **287**:321–324.
117. Jansa SA, Lundrigan BL, Tucker PK. Tests for positive selection on immune and reproductive genes in closely related species of the murine genus *Mus*. *J Mol Evol* 2003; **56**:294–307.
118. Turner LM, Hoekstra HE. Adaptive evolution of fertilization proteins within a genus: Variation in ZP2 and ZP3 in deer mice (*Peromyscus*). *Mol Biol Evol* 2006; **23**:1656–1669.
119. Swann CA, Cooper SJ, Breed WG. Molecular evolution of the carboxy terminal region of the zona pellucida 3 glycoprotein in murine rodents. *Reproduction* 2007; **133**:697–708.
120. Jégou A, Ziyyat A, Barraud-Lange V, Perez E, Wolf JP, Pincet F, Gourier C. CD9 tetraspanin generates fusion competent sites on the egg membrane for mammalian fertilization. *Proc Natl Acad Sci* 2011; **108**:10946–10951.
121. Bianchi E, Doe B, Goulding D, Wright GJ. Juno is the egg Izumo receptor and is essential for mammalian fertilization. *Nature* 2014; **508**:483–487.
122. Vicens A, Roldan ERS. Coevolution of positively selected IZUMO1 and CD9 in rodents: Evidence of interaction between gamete fusion proteins? *Biol Reprod* 2014; **90**:113.
123. Turner LM, Hoekstra HE. Reproductive protein evolution within and between species: Maintenance of divergent ZP3 alleles in Peromyscus. *Mol Ecol* 2008; **17**:2616–2628.
124. Cherr GN, Yudin AI, Katz DF. Organization of the Hamster Cumulus Extracellular Matrix: A hyaluronate-glycoprotein gel which modulates sperm access to the oocyte: Extracellular matrix/hyaluronate/oocyte-cumulus complex/extracellular matrix glycoproteins/sperm enzymes. *Dev Growth Differ* 1990; **32**:353–365.
125. Messner CB, Demichev V, Wendisch D, Michalick L, White M, Freiwald A, Textoris-Taube K, Vernardis SI, Egger A-S, Kreidl M, Ludwig D, Kilian C et al. Ultra-high-throughput clinical proteomics reveals classifiers of COVID-19 infection. *Cell Systems* 2020; **11**:11–24.e4.
126. Jarkovska K, Martinkova J, Liskova L, Haiada P, Moos J, Rezabek K, Gadher SJ, Kovarova H. Proteome mining of human follicular fluid reveals a crucial role of complement cascade and key biological pathways in women undergoing in vitro fertilization. *J Proteome Res* 2010; **9**:1289–1301.
127. Malm J, Sonesson A, Hellman J, Bjartell A, Frohm B, Hillarp A. The pentraxin serum amyloid P component is found in the male genital tract and attached to spermatozoa. *Int J Androl* 2008; **31**: 508–517.
128. Zhuo L, Kimata K. Structure and function of inter-$\alpha$-trypsin inhibitor heavy chains. *Connect Tissue Res* 2008; **49**:311–320.
129. Biardi JE, Ho CY, Marcinczyk J, Nambiar KP. Isolation and identification of a snake venom metalloproteinase inhibitor from California ground squirrel (*Spermophilus beecheyi*) blood sera. *Toxicon* 2011; **58**:486–493.
130. Gibbs HL, Sanz L, Pérez A, Ochoa A, Hassinger ATB, Holding ML, Calvete JJ. The molecular basis of venom resistance in a rattlesnake-squirrel predator-prey system. *Mol Ecol* 2020; **29**: 2871–2888.
131. Firman RC, Gomendio M, Roldan ER, Simmons LW. The coevolution of ova defensiveness with sperm competitiveness in house mice. *Am Nat* 2014; **183**:565–572.
132. Paczkowski M, Krisher R. Aberrant protein expression is associated with decreased developmental potential in porcine cumulus-oocyte complexes. *Mol Reprod Dev* 2010; **77**:51–58.

133. Nagy A, Gertsenstein M, Vintersten K, Behringer R. *Manipulating the mouse embryo*. Cold Spring Harbor, New York: Cold Spring Harbor Laboratory Press; 2003.
134. Vandenbergh JG. Effect of the presence of a male on the sexual maturation of female mice. *Endocrinology* 1967; **81**:345–349.
135. Bronson FH. The reproductive ecology of the house mouse. *Q Rev Biol* 1979; **54**:265–299.
136. Chang PL, Kopania E, Keeble S, Sarver BAJ, Larson E, Orth A, Belkhir K, Boursot P, Bonhomme F, Good JM, Dean MD. Full exome sequencing of wild derived inbred strains of mice reveals a rich source of novel genetic variants. *Mamm Genome* 2017; **28**:416–425.
137. Dean MD, Nachman MW. Faster fertilization rate in conspecific versus heterospecific matings in house mice. *Evolution* 2009; **63**: 20–28.